CONF-9610236--1

UCRL-JC-125076
Preprint

Models and Applications of the UEDGE Code

M.E. Rensink, D.A. Knoll, G.D. Porter, T.D. Rognlien, G.R. Smith, and F. Wising

This paper was prepared for submittal to

IAEA Technical Committee Meeting on Advances in Computer
Modeling of Fusion Plasmas
Los Angeles, CA, October 2-4, 1996

September 30, 1996

Models and Applications of the UEDGE Code

M. E. Rensink, D. A. Knoll[†], G. D. Porter, T. D. Rognlien, G. R. Smith, F.Wising[††]

Lawrence Livermore National Laboratory, Livermore, CA, USA
[†]Idaho National Engineering Laboratory, Idaho Falls, ID, USA
[††]Chalmers University of Technology, Gothenburg, Sweden

1. Introduction

The transport of particles and energy from the core of a tokamak to nearby material surfaces is an important problem for understanding present experiments and for designing reactor-grade devices. A number of fluid transport codes [1-4] have been developed to model the plasma in the edge and scrape-off layer (SOL) regions. This report will focus on recent model improvements and illustrative results from the UEDGE code. Some geometric and mesh considerations are introduced in Section 2, followed by a general description of the plasma and neutral fluid models in Section 3. A few comments on computational issues are given in Section 4. Two important applications are illustrated in Section 5 (benchmarking) and Section 6 (the ITER radiative divertor). The last two sections report on some recent work to improve the models in UEDGE by coupling to a Monte Carlo neutrals code and by utilizing an adaptive grid.

2. Geometry

The spatial domain is toroidally symmetric with variations in the two-dimensional poloidal plane. The multiply-connected domain includes some of the closed magnetic flux surfaces in the core near the separatrix and the open magnetic flux surfaces in the SOL and private flux regions. We use quadrilateral cells with one of the coordinates, x, aligned along poloidal magnetic flux surfaces; the second coordinate, y, is often oriented along surfaces orthogonal to the flux surfaces, but for UEDGE the second coordinate surfaces can be at arbitrary angles with respect to the flux surfaces, so irregular material boundaries can be modeled. The poloidal magnetic flux surfaces are obtained from the output of an MHD equilibrium code such as EFIT or TEQ. We specify the number of cells in the x and y directions and the spatial distribution of the cells along some reference surfaces, e.g., the separatrix and the outboard midplane. The mesh for a typical lower single-null DIII-D configuration is shown in Figure 1.

3. Physics Model

The model solves the classical Braginskii plasma fluid equations for transport along the magnetic field, **B**, and assumes anomalous diffusive transport across **B**. The plasma fluid variables are the density for each ion charge state, electron temperature and composite ion+neutral temperature. Both parallel and perpendicular fluxes can be flux-limited. The electrostatic potential is obtained from the charge conservation equation with parallel current from the inertialess electron momentum equation (parallel Ohm's law) and perpendicular current from either anomalous conductivity or the toroidal angular momentum equation [31]. Ions striking the divertor plate are recycled as atomic neutrals at the local ion thermal energy. The neutral gas that recycles from the divertor plate is modeled by fluid equations where inertial is retained in the parallel direction along **B**. In comparisons with a more

complete Navier-Stokes neutral gas model, this reduced Navier-Stokes model has been shown to accurately represent the ion-neutral momentum exchange and the collisonally enhanced momentum and energy transport including neutral-neutral collisions. A simpler diffusive gas model is also available in the code. The parallel flow velocity of the multi-charge-state impurities is described by force balance equations for each charge state or by the FMOMBAL package which solves for the mass-averaged flow velocity and includes some higher-order-velocity-moment effects. Atomic data for hydrogen rates of excitation, ionization and recombination is taken from results of a collisional-radiative model by Stotler. The data for impurity rates is derived from results of either the STRAHL or ADPAK codes, using a package developed by Braams. The boundary conditions at the core-edge interface are typically fixed density and temperatures (or heat fluxes). A sheath condition relates the particle and heat fluxes incident on the divertor plate. Ion recycling coefficients at the divertor plate and neutral albedos at the walls are specified by the user.

4. Numerical Methods

The fluid equations are spatially discretized using finite-volume differencing. The non-orthogonal mesh algorithm in UEDGE uses a general 9-point difference stencil which preserves the magnetic flux surfaces as one coordinate to resolve the highly anisotropic transport along and across **B**. A fully implicit formulation of the fluid equations is used to obtain either time-dependent or steady state solutions. We use a numerically computed Jacobian for pre-conditioning in both the Newton-Krylov solver (nksol) and the method-of-lines time-dependent solvers (daspk and vodpk).

5. Benchmarking with Experimental Data

The validity of the physics models in UEDGE is tested by comparing the simulation results with experimental data. Such code validation is necessary in order to have confidence in the model predictions for future devices such as ITER. The DIII-D experiment has an extensive set of divertor plasma diagnostics which allows one to determine some free parameters in the model and make detailed comparisons with plasma profiles. In the UEDGE model, the power input to the SOL from the core plasma and the plasma density at the separatrix are set directly from experimental measurements. The anomalous radial transport parameters in the model are adjusted to obtain a good fit to the measured plasma density and temperature profiles at the outboard midplane, as shown in Figure [2]. One can obtain information about the variation of radial transport parameters by simulating many different experimental conditions, as shown in Figure [3]. These results indicate that the electron thermal diffusivity is larger in L-mode than in H-mode plasmas, and it increases with the power input to the SOL. In both the experiment and the simulation results we observe a thermal collapse or plasma detachment phenomenon when the divertor plate temperature falls below about 2 eV. Below this temperature, the plasma cannot efficiently ionize the recycling neutrals from the divertor plate. Figure [4] shows the operational boundaries for plasma detachment in DIII-D as determined by a series of UEDGE simulations. At the highest input power, the plasma is attached at both divertor plates. At moderate input power, the plasma is detached at the inner divertor plate only. At lower input power, the plasma is detached at both inner and outer divertor plates. Higher density tends to shift the transition boundaries toward lower power. This general picture of detachment is in agreement with the DIII-D experimental observations. The specific position of the boundaries in the UEDGE simulations may vary somewhat with other parameters such as the radial transport coefficients.

6. ITER Radiative Divertor

A critical problem for next generation fusion reactors is the high heat flux on walls and divertor plates

surrounding the core plasma. The ITER design reduces the heat flux by radiating a significant fraction of the power in the SOL before it reaches the divertor plates. The heat flux that does strike the plate is further reduced by tilting the plate with respect to the poloidal magnetic flux surfaces so as to spread the heat flux over a larger area. Simulations of ITER with the UEDGE code demonstrate both techniques for reducing the heat flux.

Tilting a divertor plate modifies the plasma density and temperature profiles on the plate as shown in Figure [5]. The tilted plate directs the recycling neutrals toward the separatrix where they are ionized, increasing the plasma density and decreasing the temperature near the strike point; conversely, on the outboard side of the strike point the density decreases and the temperature increases. The net effect of these profile changes is that the peak heat load on the divertor plate decreases somewhat faster than the geometric increase in the exposed surface area, as shown in Figure [6]. Tilting the plate also changes the hydrogenic flow pattern which has a significant impact on the distribution of impurity ions caught in the flow near the plates.

Radiative losses in the SOL can be increased beyond the natural hydrogenic losses by injecting various impurities such as neon or argon. UEDGE simulations of ITER with a low concentration of neon, e.g., 0.4 percent at the core boundary, indicate that a significant fraction of the power input to the SOL can be radiated by the impurities. For these simulations we specify the Ne^{+8} concentration at the core boundary and assume 100 percent recycling of neon at the walls and divertor plate. Neon neutrals originating at the plate are modeled with a simple diffusive transport model. The distribution of the neon and associated radiation in the SOL is strongly affected by the hydrogenic flow and the strength of the radial diffusion for the impurity ions. Figure [7] compares the neon radiation for two cases with orthogonal divertor plates: weak diffusion ($D_\perp$=0.33 m^2/sec) and strong diffusion ($D_\perp$=0.67 m^2/sec). It shows that for weak diffusion the neon radiation is spread more or less uniformly throughout the entire length of the SOL whereas for strong diffusion the neon radiates mostly above the x-point. If the divertor plate is tilted, the neon is distributed more uniformly due to strong hydrogenic flows induced in the SOL.

7. Coupling to a Monte Carlo Neutrals Code

When the neutral mean free path exceeds the gradient scale length of the background plasma, the validity of the diffusive and inertial fluid neutrals models becomes questionable. In the long mean free path regime, neutrals can be accurately and efficiently described by a Monte Carlo neutrals model. We have used the UEDGE plasma model in combination with the EIRENE Monte Carlo neutrals code to simulate a divertor plasma. We use a time-dependent simulation method, illustrated schematically in Figure [8], with UEDGE and EIRENE running sequentially in a cycle that is repeated until the plasma has reached a steady state. We find that the time step size is limited to $dt \leq 5\times10^{-6}$ sec by stability constraints of the explicit coupling algorithm, as shown in Figure [9]. The time scale for reaching steady state is several milliseconds, or about 1000 time steps. The self-consistent steady states from the purely fluid UEDGE neutrals model and from the EIRENE Monte Carlo neutrals model are very similar as shown in Figure [10]. There are significant differences in the atomic hydrogen neutral densities very close to the divertor plate where molecular effects (not included in UEDGE) are expected to be important.

8. Adaptive Mesh for Improved Spatial Resolution

An adaptive mesh capability allows one to alter the spatial gridding so as to resolve strong local gradients that may develop during a simulation. Some initial steps toward this capability have been

implemented in UEDGE. The sharply defined ionization-recombination front associated with a detached plasma provides the motivation. An example of such an ionization front in a simple box-like geometry is shown in Figure [11] which displays the ion particle source rate in the region near a divertor plate. Ions flow toward the plate and are recycled as neutrals flowing away from the plate. The ionization front where the neutrals are strongly attenuated is located on each flux surface near the point where the electron temperature is about 2 eV. The poloidal extent of the ionization front is only about .02 m along the separatrix. For simulation of attached plasmas, the poloidal cell size is smallest at the divertor plate and increases upstream toward the x-point. If the plasma detaches, the ionization front moves upstream into the coarser mesh region. When this occurs we have the option of redistributing the mesh points along each magnetic flux surface so as to concentrate them near the point on the flux surface where the ionization source is a maximum. Figure [12] shows the original and modified meshes generated by UEDGE. The radiation losses from the ionization-recombination front are shown in Figure [13] on these two meshes. The two distinct peaks are associated separately with ionization and recombination processes which are most efficient at higher and lower temperatures respectively. The poloidal extent of the upstream ionization peak is reduced with the modified mesh which allows steeper gradients to be resolved.

Summary

UEDGE is a comprehensive two-dimensional fluid transport code for modeling edge plasmas in tokamaks. The model encompasses a variety of plasma and atomic physics, complicated divertor plate geometries and multi-species impurities. The model results have been benchmarked against experimental data from DIII-D and applied to the design of reactor-grade devices like ITER. Progress on coupled fluid-plasma and Monte-Carlo-neutral models has been demonstrated. Meshes can be modified in response to localized plasma features to yield better spatial resolution without increasing the total number of mesh points. Work is also in progress on self-consistent coupling with a core plasma transport code [39].

Acknowledgments

The EIRENE code and many useful suggestions for its use were supplied by David Coster of the Max-Planck Institut für Plasmaphysik in Garching.

This work was performed under the auspices of the United States Department of Energy under contract numbers W-7405-ENG-48 at LLNL, DE-AC07-94ID13223 at INEL, and DE-FG02-91-ER-54109 at MIT.

References

[1] general UEDGE references

[2] general B2 reference

[3] general B2-EIRENE reference

[4] general EDGE2D-NIMBUS reference

[31] Rognlien, T.D., Mattor, N., and Cohen, R.H., Bull. Am. Phys. Soc. **40** (1995) 1881.

[39] Tarditi, A., Cohen, R.H., Craddock, G.J., Crotinger, J.A., Rognlien, T.D., Shestakov, A.I., and Smith, G.R., Contributions to Plasma Physics **36** (1996) .

Figures

[1] Mesh configuration for typical DIII-D lower single-null simulation. The dashed line shows the position of the wall, divertor plate, bias ring and baffle in DIII-D.

[2] Density and temperature profiles at the outboard midplane from DIII-D experimental data and from a UEDGE simulation with radial transport coefficients chosen to best fit the data.

[3] Variation of the thermal diffusivity with input power in DIII-D for L-mode and ELMing H-mode as determined by fitting UEDGE simulation results to experimental data.

[4] Operational boundaries for detached plasma regimes in UEDGE simulations of DIII-D.

[5] The plate tilt angle is defined relative to a plate whose surface is orthogonal to the poloidal magnetic flux surfaces. The plasma density and temperature profiles are from simulations of the ITER outer divertor with various plate tilt angles.

[6] Peak heat load on the divertor plate decreases with increasing plate tilt angle. The total absorbed heat load is the sum of electron and ion heat fluxes and the contribution due to electron-ion recombination at the plate.

[7] Contours of neon radiation in the outer SOL for cases with weak and strong radial diffusion. The neon concentration at the core boundary is 0.2 percent. Divertor plates are orthogonal to the poloidal magnetic flux surfaces.

[8] Schematic of UEDGE coupling to EIRENE Monte Carlo neutrals code

[9] Short term evolution of total radiated power for various time steps

[10] Contours of atomic neutral density in the divertor from UEDGE fluid model and from EIRENE Monte Carlo neutrals model.

[11] Contours of electron temperature and ion particle source due to ionization of neutrals originating at the divertor plate. The ions are flowing from left to right toward the plate, where they are recycled as neutrals flowing from right to left away from the plate. The plasma is detached in the sense that the peak of the ionization occurs some finite distance upstream rather than directly in front of the plate.

[12] Original (orthogonal) mesh and modified mesh with improved resolution near the ionization front

[13] Contours of hydrogenic radiation from simulations on the orthogonal mesh and modified mesh. The upstream peak is associated with ionizatio;n; the downstream peak is due to recombination.

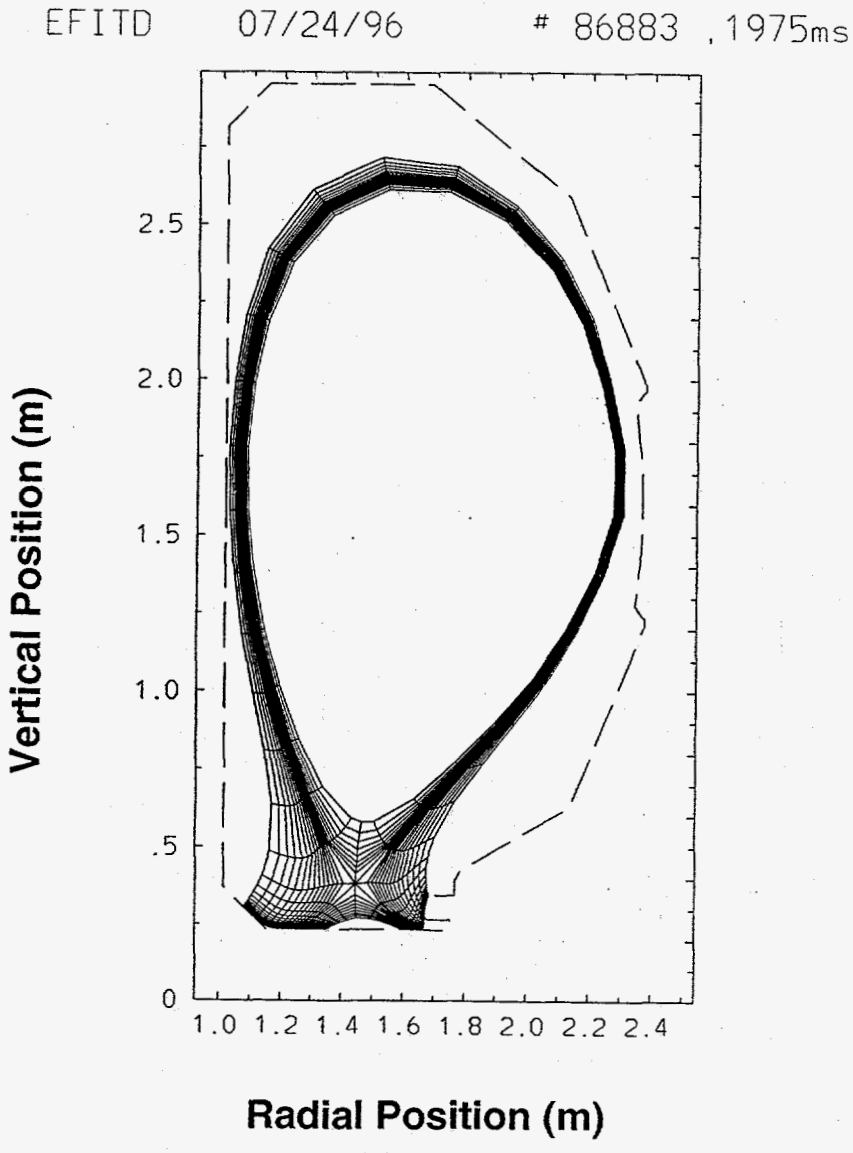
EFITD 07/24/96 # 86883 ,1975ms
Vertical Position (m)
2.5
2.0
1.5
1.0
.5
0
1.0 1.2 1.4 1.6 1.8 2.0 2.2 2.4
Radial Position (m)

figure 1

- $D_\perp = 0.3\ m^2/s; \chi_e = 1.4\ m^2/s; \chi_i = 1.5\ m^2/s$

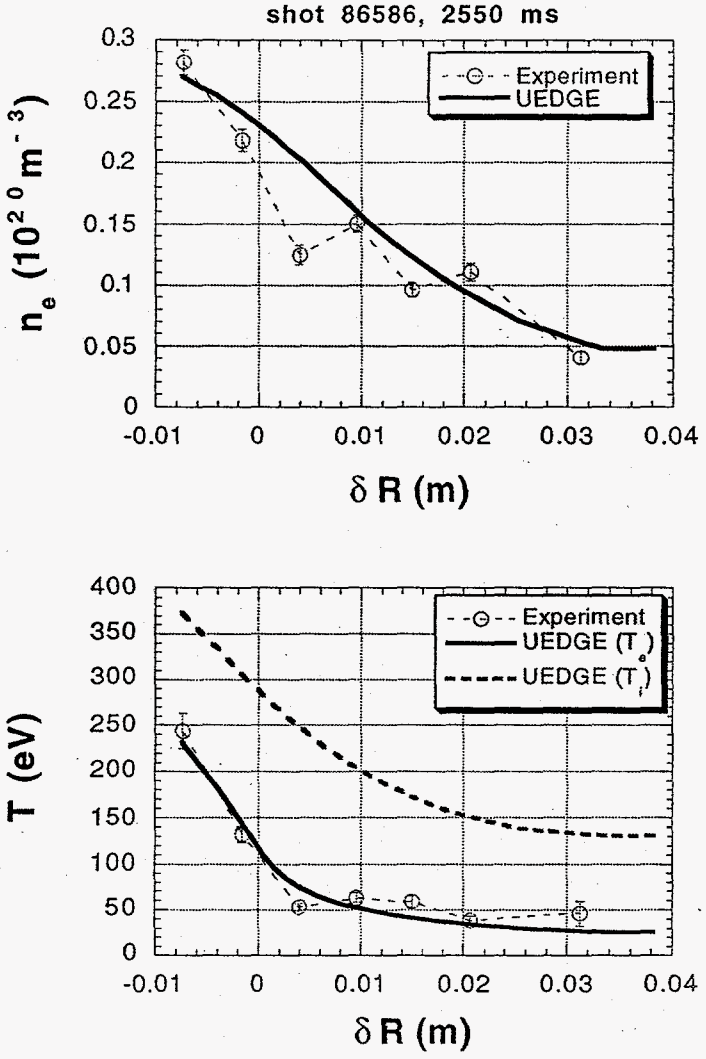

Figure 2

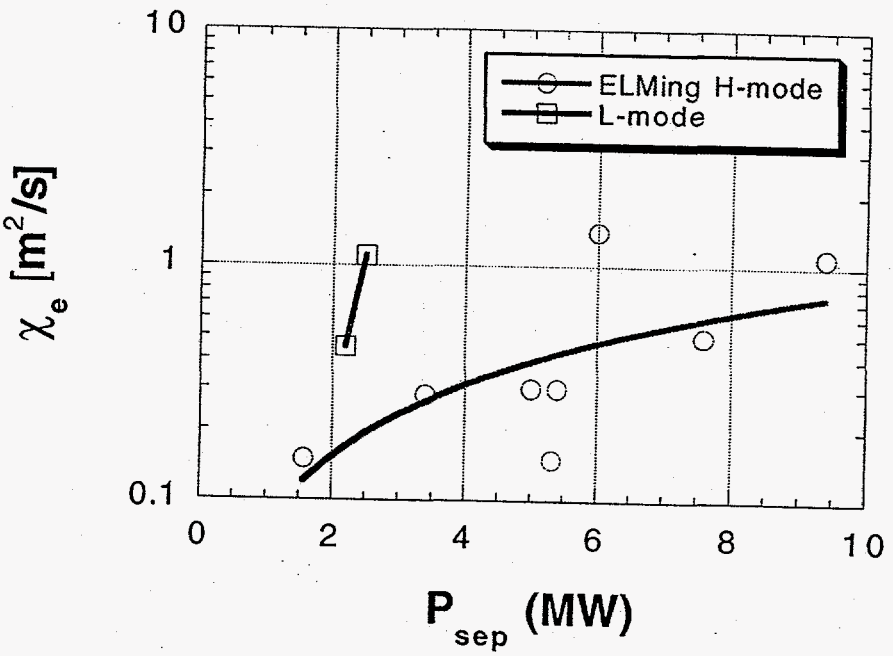

Figure 3

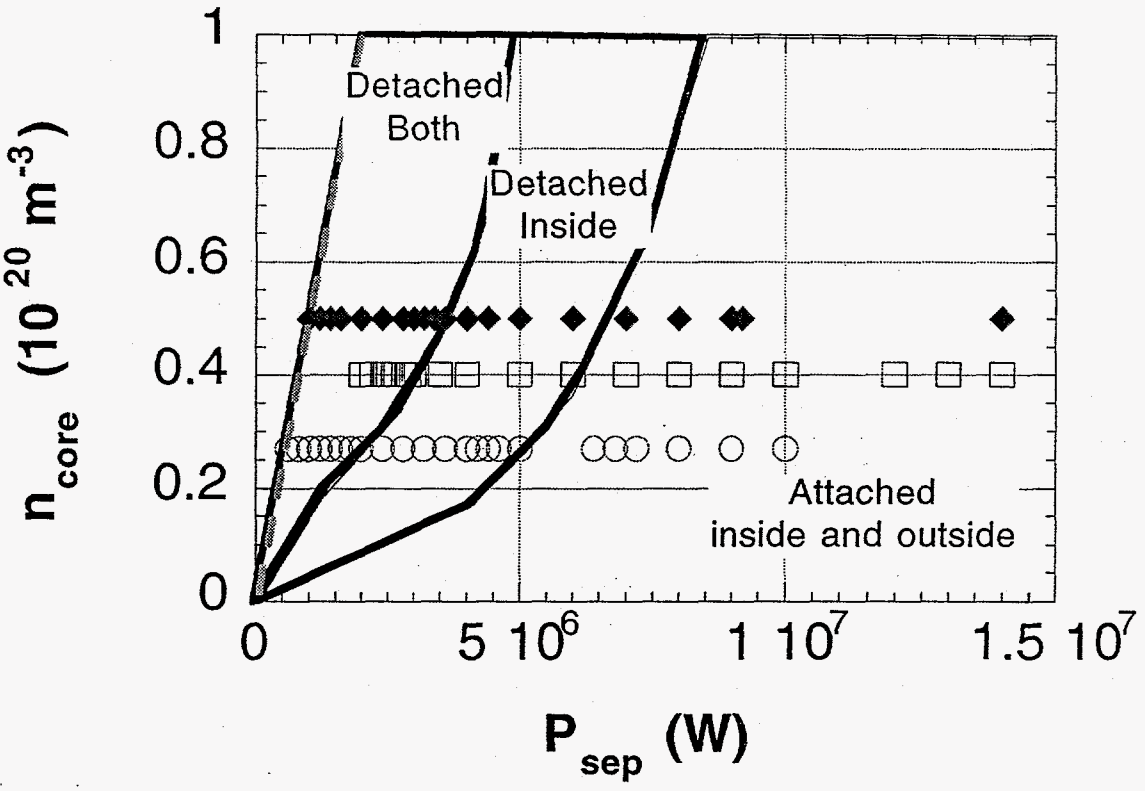
1
0.8
0.6
0.4
0.2
0
n_{core} (10^{20} m^{-3})
Detached
Both
Detached
Inside
Attached
inside and outside
0
5 10^6
1 10^7
1.5 10^7
P_{sep} (W)

Figure 4

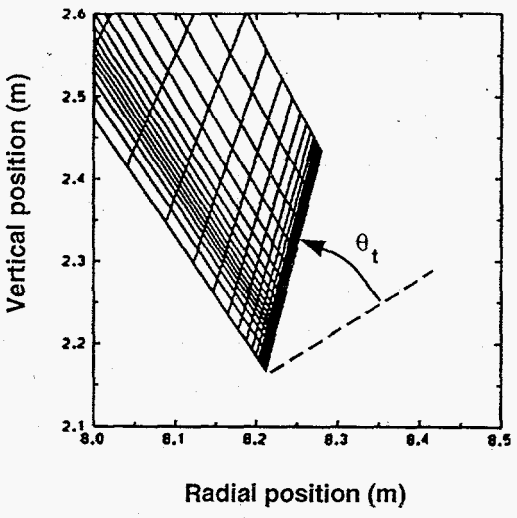
Vertical position (m)
2.6
2.5
2.4
2.3
2.2
2.1
8.0
8.1
8.2
8.3
8.4
8.5
θ_t
Radial position (m)

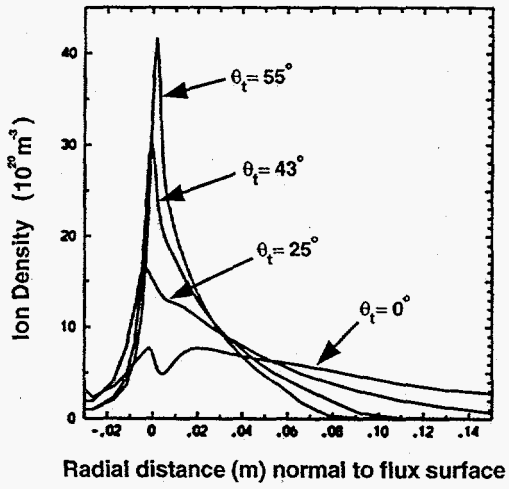
Ion Density (10^{20} m^{-3})
40
30
20
10
0
θ_t= 55°
θ_t= 43°
θ_t= 25°
θ_t= 0°
-.02
0
.02
.04
.06
.08
.10
.12
.14
Radial distance (m) normal to flux surface

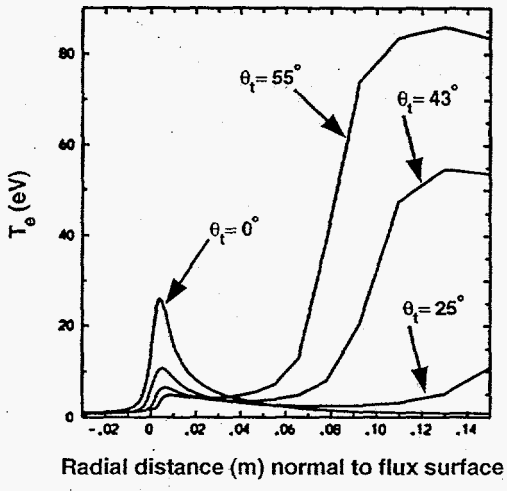
T_e (eV)
80
60
40
20
0
θ_t= 55°
θ_t= 43°
θ_t= 0°
θ_t= 25°
-.02
0
.02
.04
.06
.08
.10
.12
.14
Radial distance (m) normal to flux surface

Figure 5

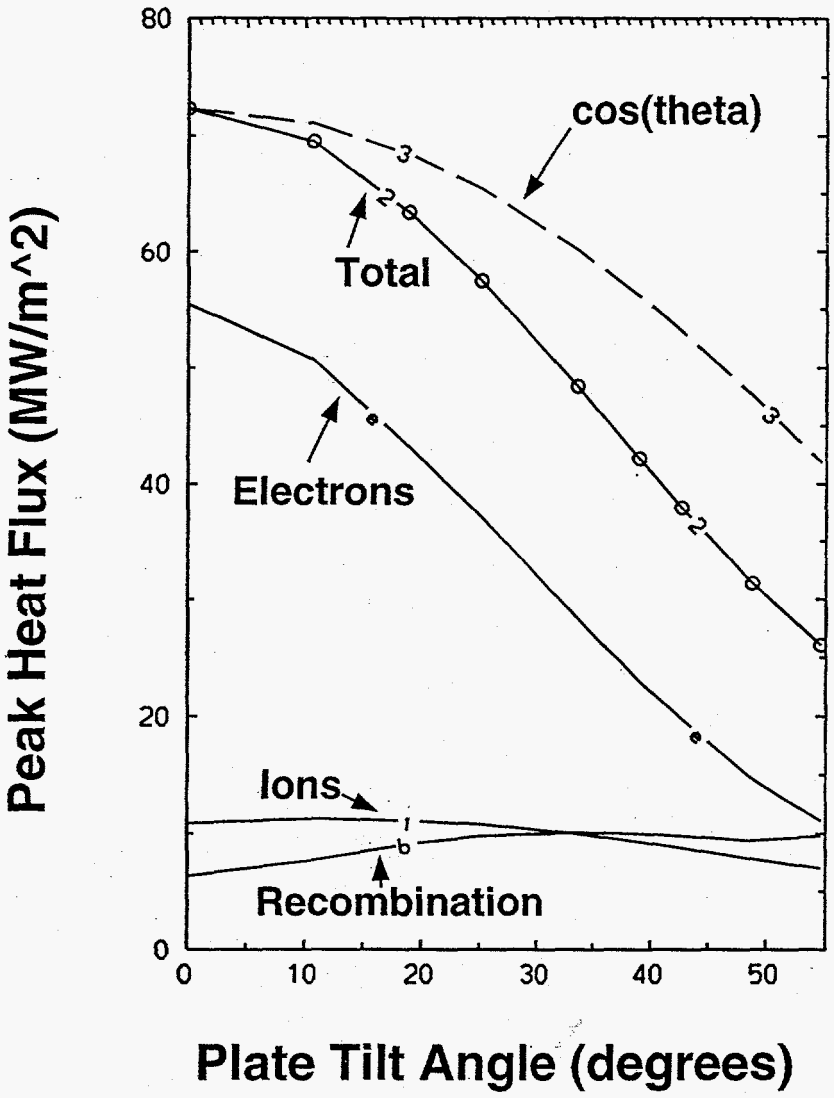
Peak Heat Flux (MW/m^2)
80
60
40
20
0
0
10
20
30
40
50
Plate Tilt Angle (degrees)
cos(theta)
Total
Electrons
Ions
Recombination
3
2
2
3
1
b

Figure 6

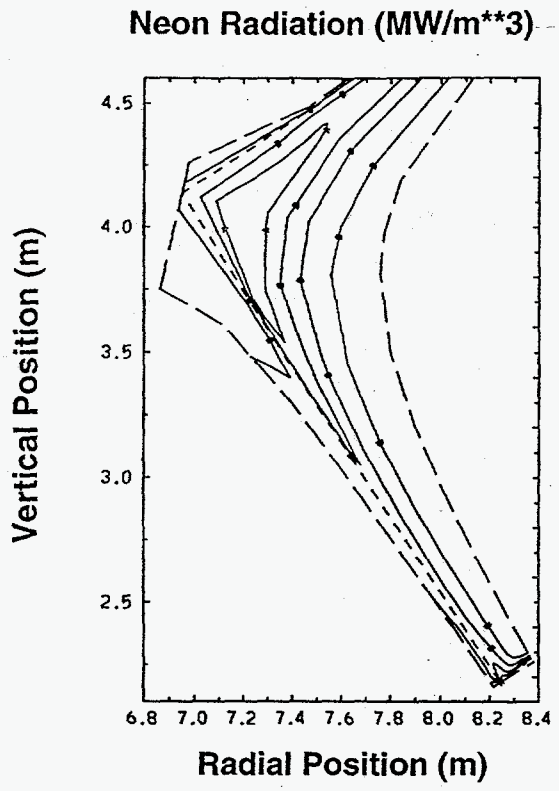

Weak Diffusion

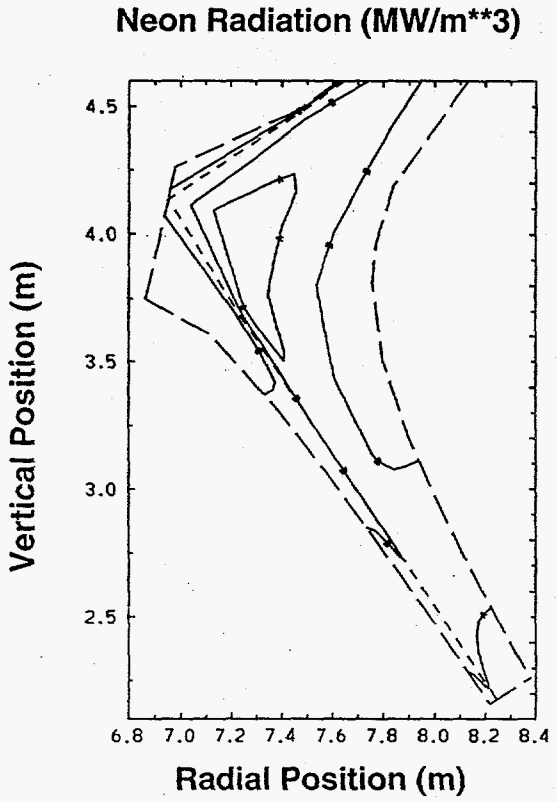

Strong Diffusion

Figure 7

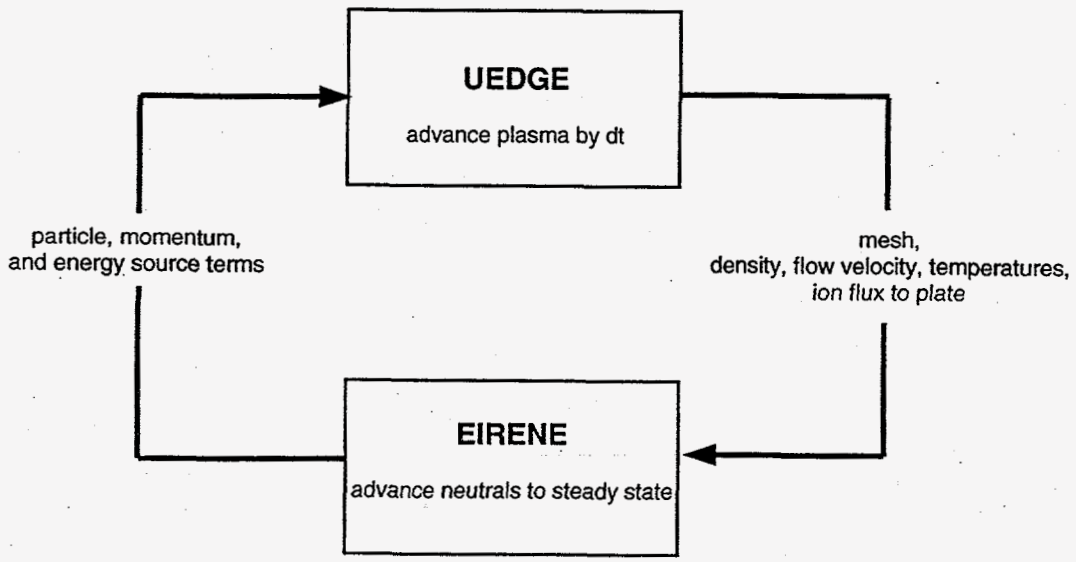
UEDGE
advance plasma by dt
particle, momentum,
and energy source terms
mesh,
density, flow velocity, temperatures,
ion flux to plate
EIRENE
advance neutrals to steady state

Figure 8

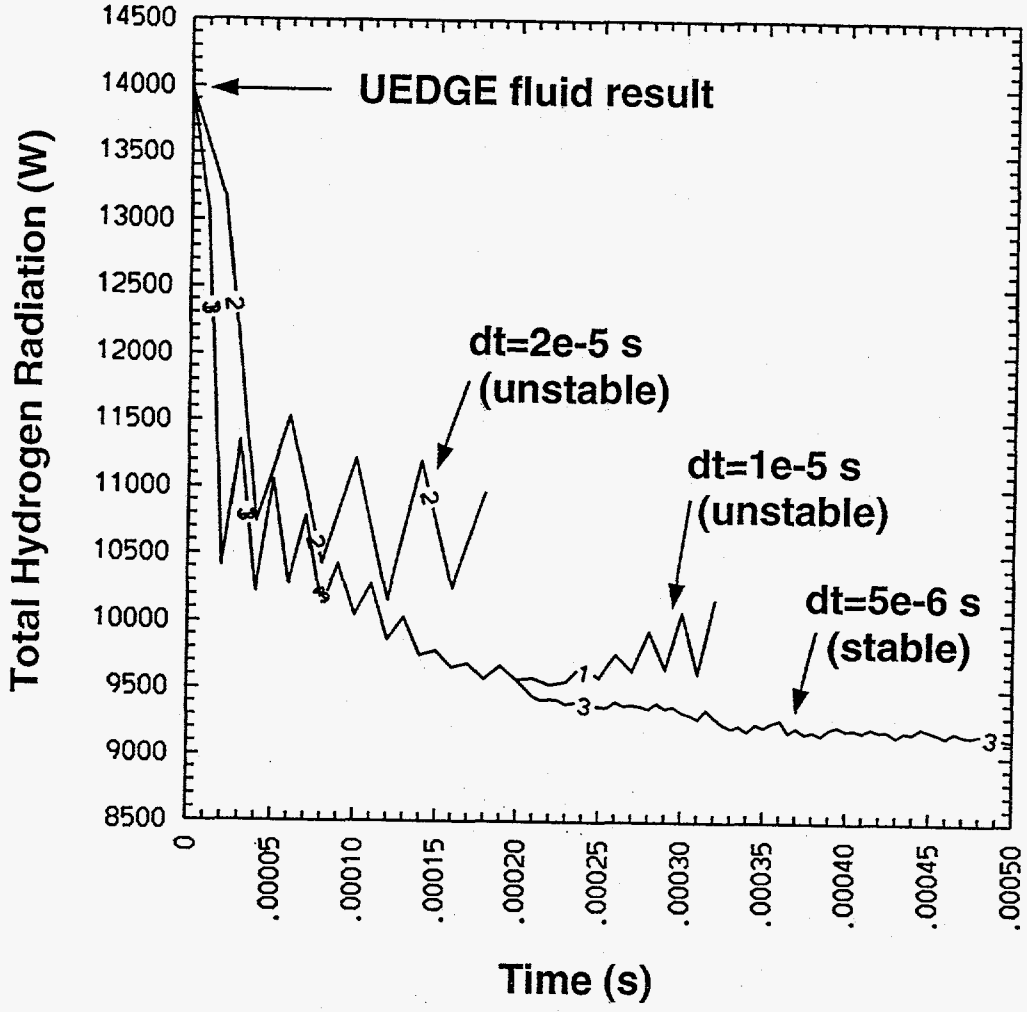
Total Hydrogen Radiation (W)
14500
14000
13500
13000
12500
12000
11500
11000
10500
10000
9500
9000
8500
0
.00005
.00010
.00015
.00020
.00025
.00030
.00035
.00040
.00045
.00050
Time (s)
UEDGE fluid result
dt=2e-5 s
(unstable)
dt=1e-5 s
(unstable)
dt=5e-6 s
(stable)

Figure 9

Atomic Neutral Density (1e20 /m^3)

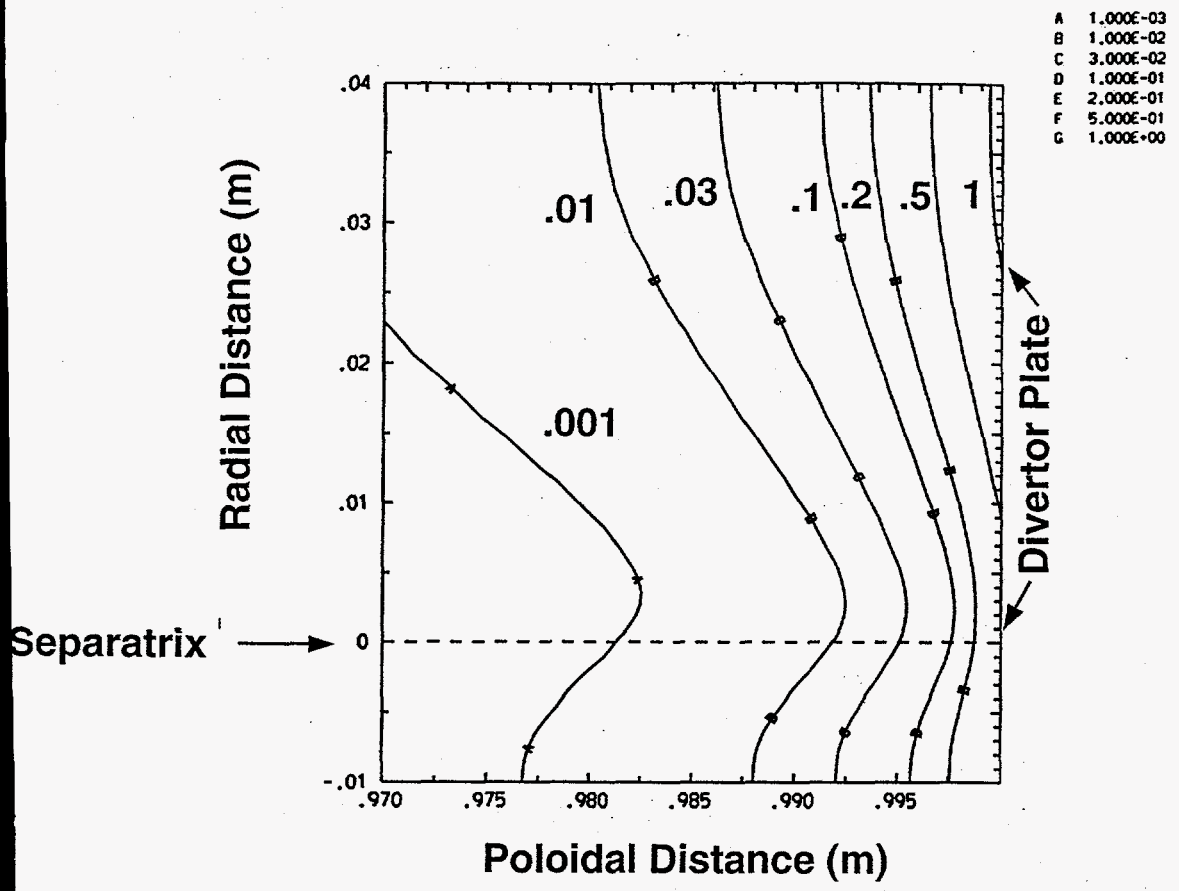

FLUID MODEL

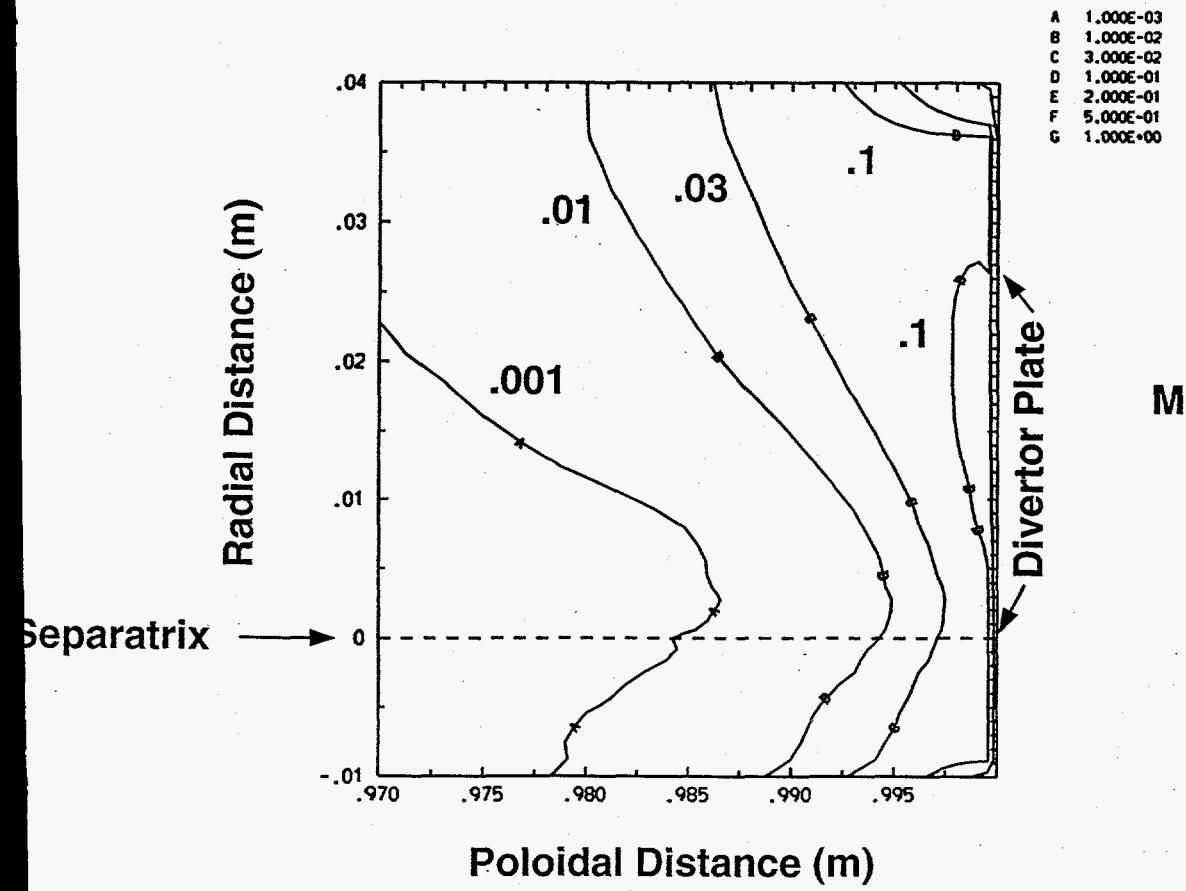

MONTE CARLO MODEL

Figure 10

Electron Temperature (eV)

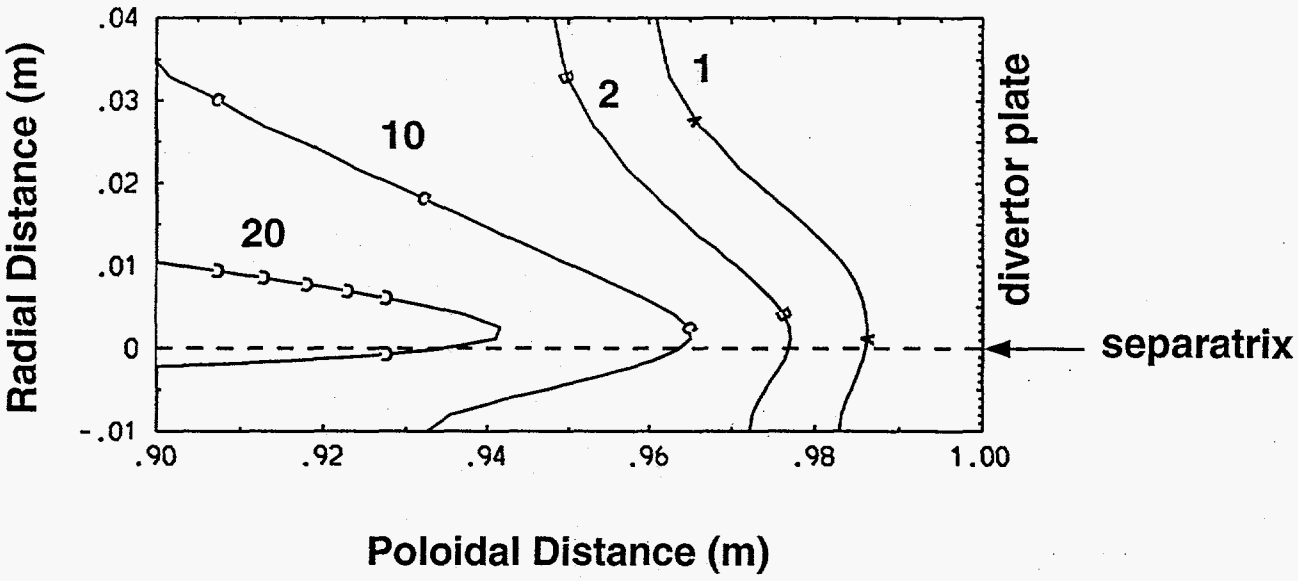

Ionization Source (1e24 part/sec/m**3)

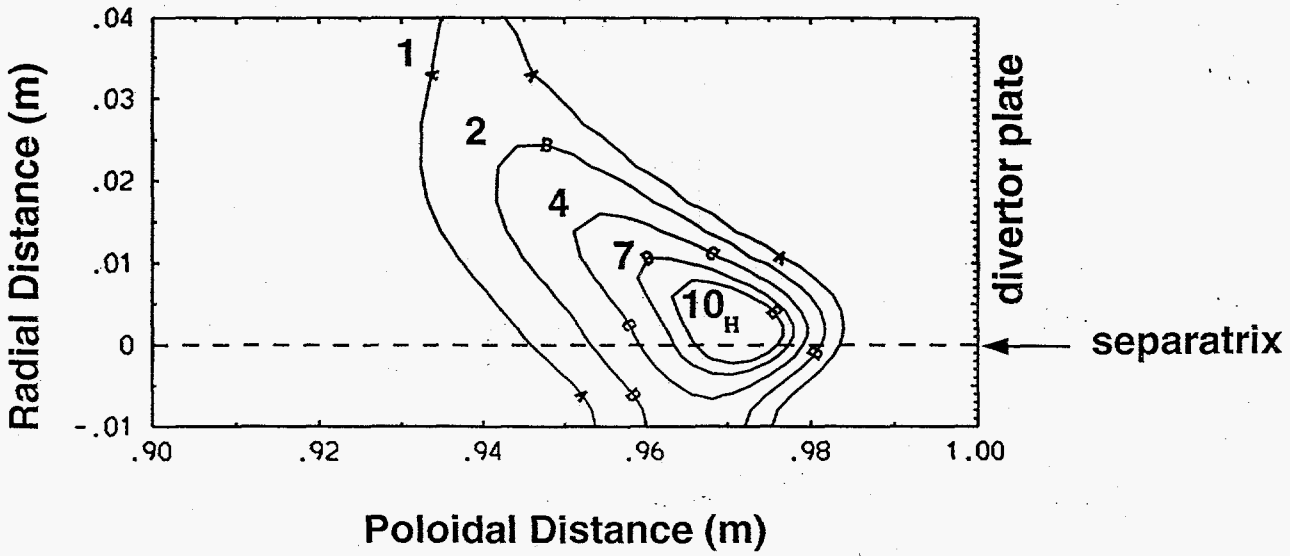

Figure 11

Slab Geometry

Orthogonal Mesh

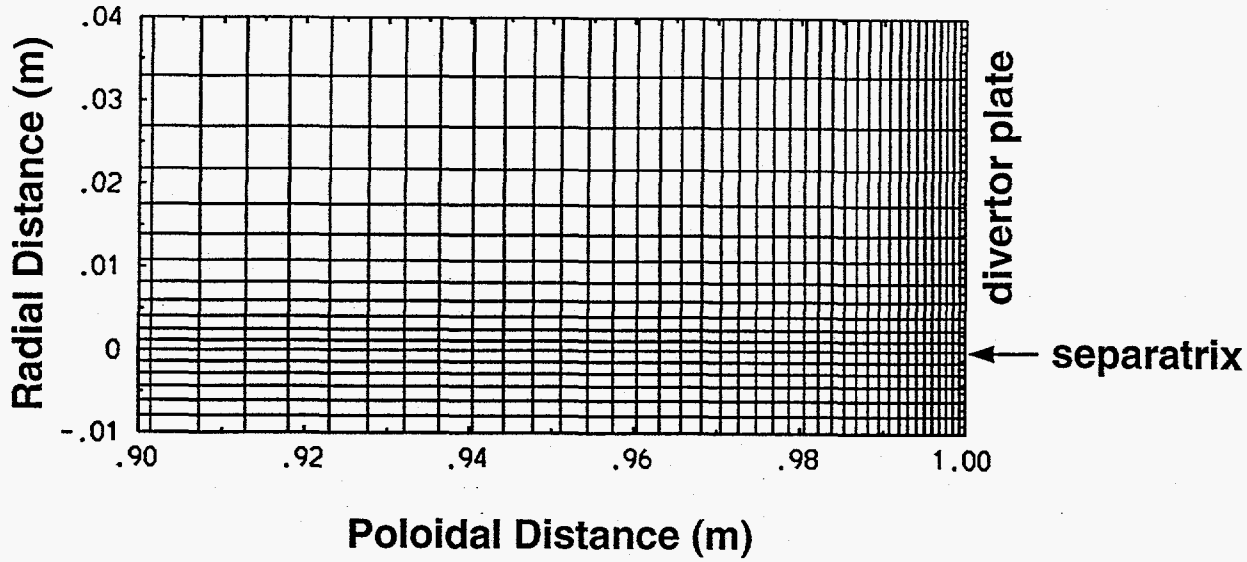

Adaptive Mesh

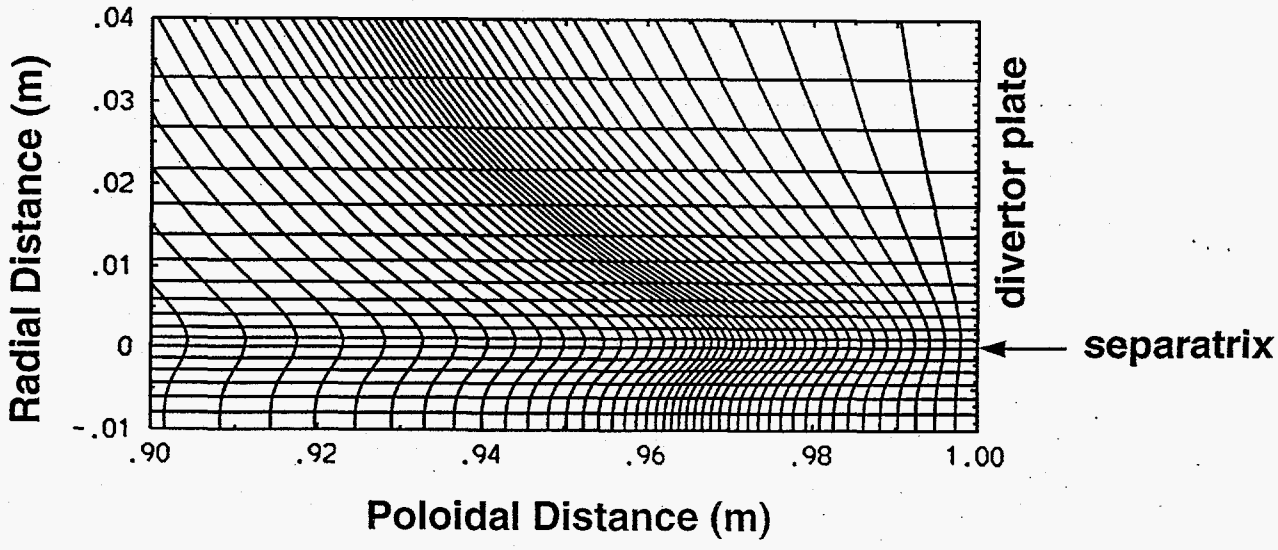

Figure 12

Hydrogenic Radiation (MW/m**3)

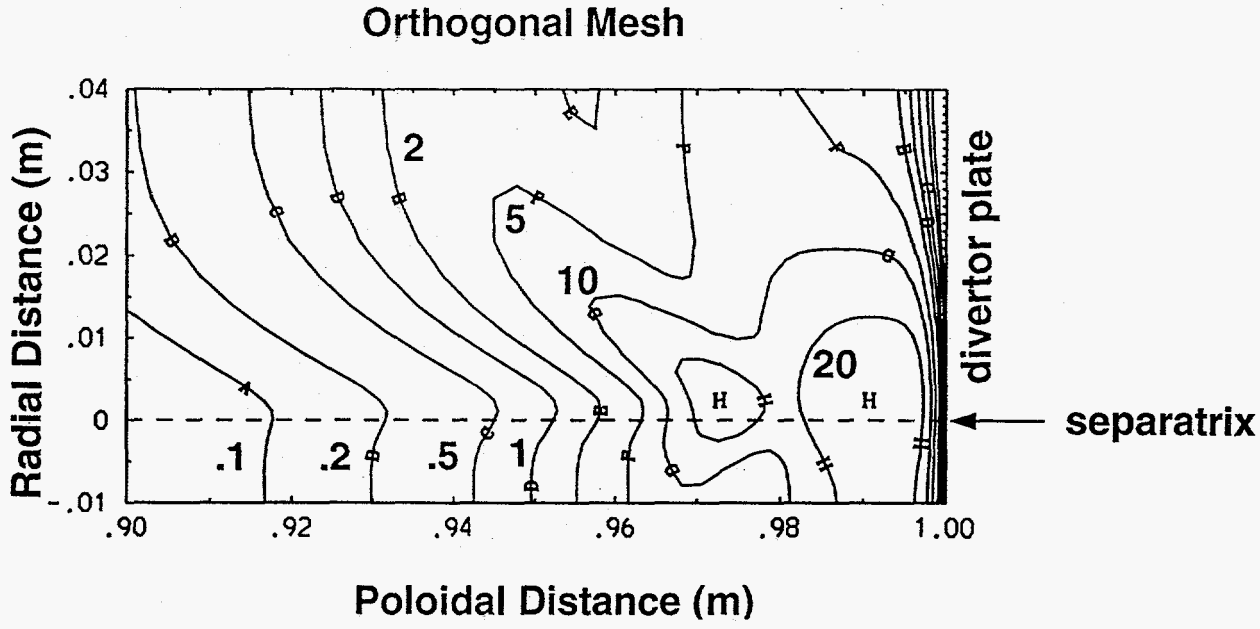

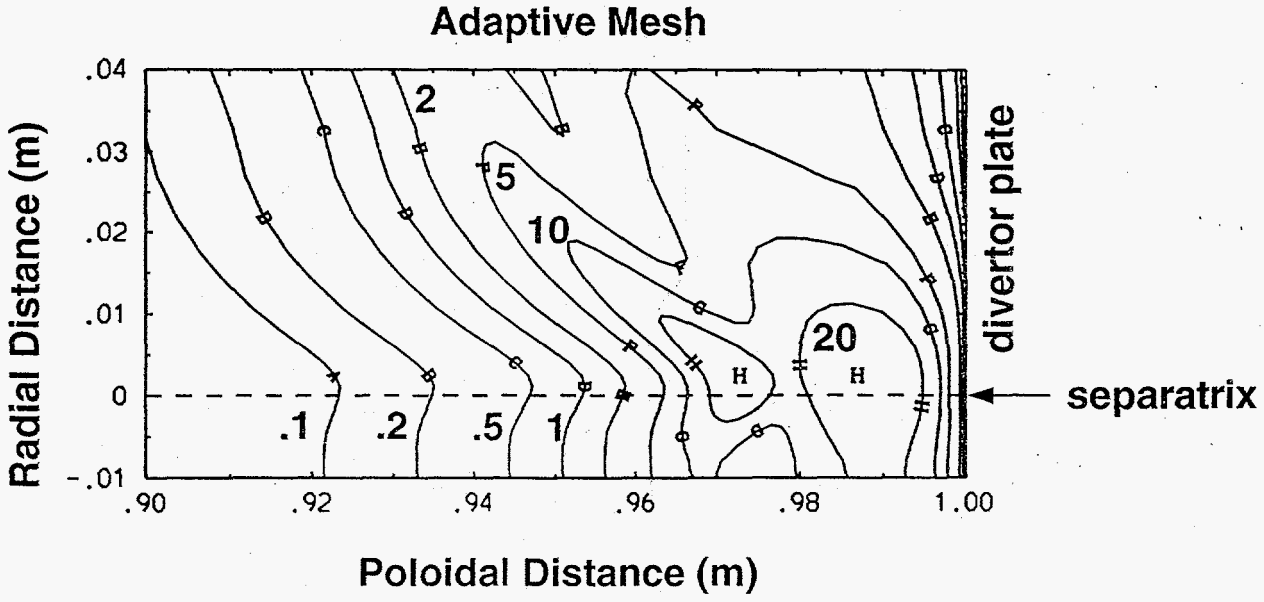

Figure 13